

# Catalyst-free MOCVD growth of ZnO nanorods and their structural characterization

HYOUN WOO KIM\*, NAM HO KIM, JAE-HYUN SHIM, NAM-HEE CHO,  
CHONGMU LEE

*School of Materials Science and Engineering, Inha University, Incheon 402-751, Korea*  
E-mail: hwkim@inha.ac.kr

We have synthesized ZnO nanorods on ZnO-coated Si(100) substrates without a metal catalyst by a reaction of a diethylzinc (DEZn) and oxygen (O<sub>2</sub>) mixture. By adjusting the argon (Ar)/O<sub>2</sub> gas flow ratio, we have obtained ZnO nanorods of various densities at a temperature of 450 °C. The ZnO nanorods had an average diameter of 30–70 nm, and transmission electron microscopy (TEM) showed a single crystalline structure.

© 2005 Springer Science + Business Media, Inc.

## 1. Introduction

In recent years, one-dimensional nanoscale materials have received considerable attention due to their remarkable properties applied in optoelectronic and electronic devices [1, 2]. Although nanorods of various compound semiconductors such as InP, GaAs, and GaP have been studied by several researchers [3–5], zinc oxide (ZnO) is recognized as one of the most promising oxide semiconductor materials, because it has a wide bandgap of 3.37 eV at room temperature, high mechanical and thermal stabilities, and a large free exciton binding energy (60 meV).

Various methods have been developed for synthesizing the ZnO nanorods [6–12]. The preparation of ZnO nanomaterials on Si substrate will pave the way for integration of future opto-electronic devices with developed Si integrated circuit technology. Although ZnO nanorod or whiskers are grown on copper metallized Si substrates by radio frequency sputter deposition [13] and on fused silica substrates by chemical vapor deposition [14], there are rare reports of the growth of ZnO nanorod on Si substrates.

In this paper, we deposit ZnO on bare Si substrates by a simple metal organic chemical vapor deposition (MOCVD) technique, using a diethylzinc (DEZn) and oxygen (O<sub>2</sub>) system. The growth of ZnO nanorods occurs through the nucleation on a continuous ZnO film that initially grows on the Si. We investigate the structural properties of the as-deposited ZnO as function of the Ar/O<sub>2</sub> gas flow ratio.

## 2. Experimental

ZnO was deposited on *p*-type silicon with (100) orientation. The substrates were cleaned with organic solvents and dried before loading into the system. DEZn (99.9999% purity Zn(C<sub>2</sub>H<sub>5</sub>)<sub>2</sub>) and O<sub>2</sub> (99.999% purity) were used as the Zn metalorganic source and oxidizer,

respectively, and Ar was used as a carrier gas of the DEZn source. A schematic diagram of the MOCVD reactor used in our experiments is previously reported [15]. Mass flow controllers separately controlled the flow of Ar and O<sub>2</sub> gases and the gas flow ratio of Ar to O<sub>2</sub> was in the range of 0.33–4. When the Ar/O<sub>2</sub> gas flow rates were 0.33, 1, 3, and 4, respectively, the O<sub>2</sub> gas flow rates were 15, 10, 5, and 4 sccm. The substrate temperature and the total pressure, respectively, were set to 450 °C and 3.5 Torr. The deposition time was set to 10 min.

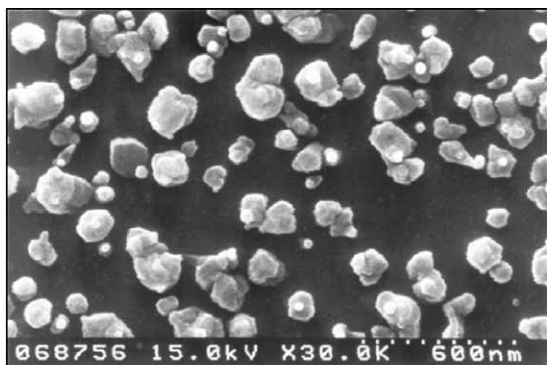
The as-grown samples were characterized by means of grazing angle X-ray diffraction (XRD: CuK<sub>α1</sub>λ = 1.5405 Å) with the incidence angle of 0.5°, scanning electron microscopy (SEM: Hitachi S4200), and transmission electron microscopy (TEM: Philips 200CM). The cross-sectional TEM sample representing the nanorods connected to the underlying film structures was prepared by Ar ion milling of polished cross-sections. The nanorods were also ultrasonically separated from the substrate by dispersing in acetone and subsequently dropped onto a porous carbon film supported on a copper grid.

## 3. Results and discussion

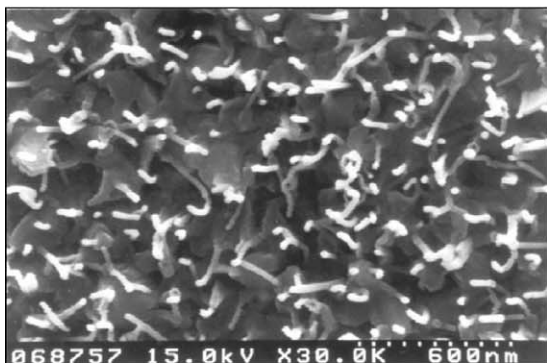
Fig. 1 shows plan-view SEM images of ZnO deposits with Ar/O<sub>2</sub> gas flow ratios of 0.33, 1, and 4, indicating that the nanostructures change from cluster-like to nanorod-like deposits with increasing Ar/O<sub>2</sub> gas flow ratio. It is clear that the Ar/O<sub>2</sub> gas flow ratio affects the morphology of ZnO deposits. The densities of the nanorods with the Ar/O<sub>2</sub> gas flow ratio of 1 and 4, respectively, increased from about  $4.6 \times 10^9$  to  $6.2 \times 10^9$  cm<sup>-2</sup>.

Fig. 2 shows cross-sectional SEM images of ZnO deposits with Ar/O<sub>2</sub> gas flow ratios of 1 and 4. The SEM images reveal that the needle-like ZnO deposits have

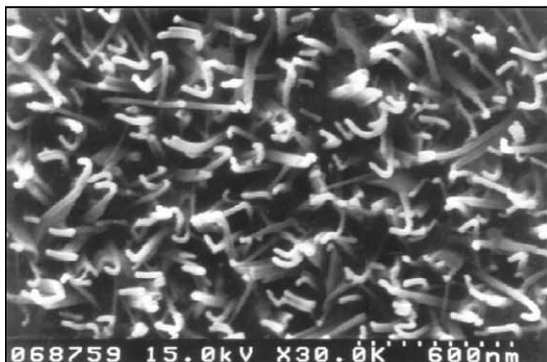
\*Author to whom all correspondence should be addressed.



(a)



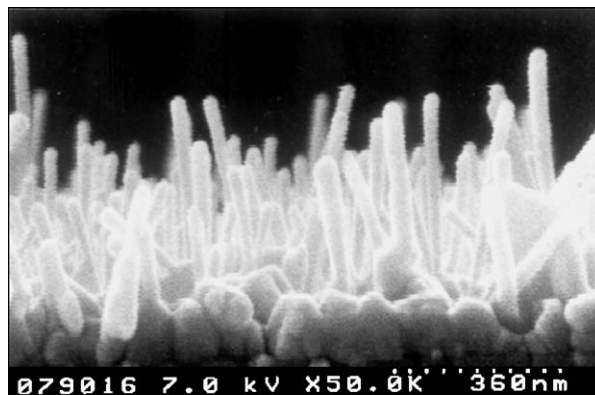
(b)



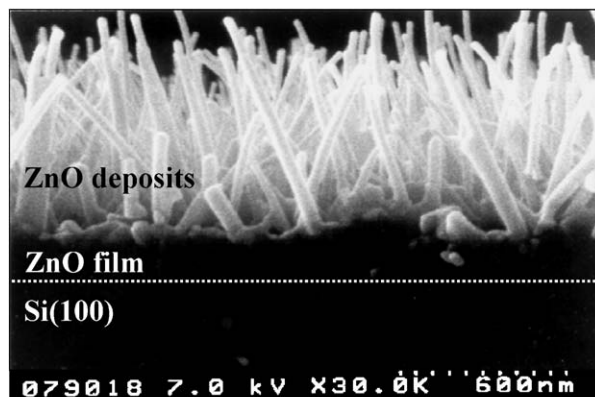
(c)

Figure 1 Plan-view SEM images of ZnO deposits grown at 450 °C with Ar/O<sub>2</sub> gas flow ratios of (a) 0.33, (b) 1, and (c) 4.

grown on top of ZnO films and that the lengths of the needle-like deposits are 300–400 and 600–700 nm, respectively. Also, the diameter of the ZnO deposits range from 30 to 70 nm. The diameter does not change but the length of the ZnO deposits increases with increasing Ar/O<sub>2</sub> gas flow ratio. The SEM images show that the needle-like deposits have grown not directly from the Si substrate but from the grains of two-dimensional ZnO material on top of the Si substrate, indicating that a thick ZnO layer has been formed in the initial deposition stage, before the formation of the nanorods. Fig. 3 shows the XRD pattern of ZnO deposits grown directly on the Si substrate with the Ar/O<sub>2</sub> gas flow ratio of 4 at 450 °C. In our XRD measurements, the angle of the incident beam to the substrate surface was about 0.5°, and a detector rotated to scan the samples. Therefore, we surmise that the peaks are mainly from the nanorods. The position of the XRD peaks shows good agreement with those of the hexagonal ZnO



(a)



(b)

Figure 2 Cross-sectional SEM images of ZnO deposits with Ar/O<sub>2</sub> gas flow ratios of (a) 1 and (b) 4.

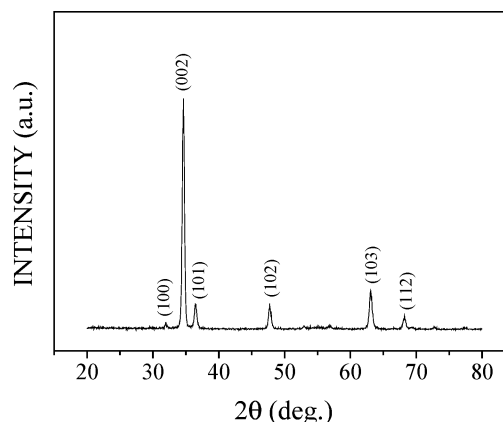
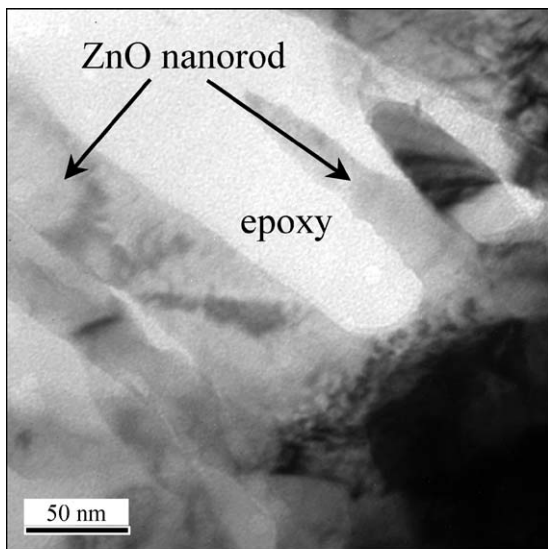


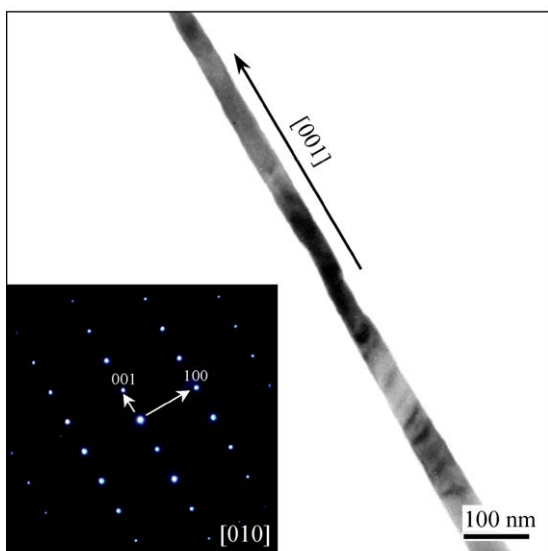
Figure 3 XRD pattern of ZnO deposits grown on Si substrate.

with lattice constants  $a = 0.3250$  and  $c = 0.5207$  nm [16].

A representative bright field TEM image in Fig. (4a) shows the general morphology of the ZnO deposits, indicating that the diameter of deposits is in the range of 30–70 nm, agreeing with the SEM images. The TEM image also indicates that the rod-like deposits have been grown on top of the pre-deposited ZnO layer, agreeing with SEM images. Fig. 4(b) is a bright field TEM image of a ZnO nanorod with a diameter of about 65 nm. The corresponding selected area electron diffraction (SAED) pattern, indicating that the long axis of this nanorod is parallel to [001] direction, can be indexed for [010] zone axis of crystalline ZnO. The reflections



(a)



(b)

Figure 4 Bright field TEM images of (a) ZnO nanorods grown on the Si substrate and (b) a ZnO nanorod. The inset shows corresponding SAED pattern recorded along the [010] zone axis.

in the SAED pattern correspond to lattice planes of bulk ZnO, indicating that the nanorod is single crystalline. The formation mechanism of the ZnO nanorods without a catalyst is currently unknown and further systematic study is necessary.

#### 4. Conclusions

In summary, we have successfully synthesized single crystalline ZnO nanorods on ZnO-coated Si substrate without catalyst using MOCVD. At a substrate temperature of 450 °C, the growth structure changes from clusters to nanorods with increasing Ar/O<sub>2</sub> gas flow ratio. At an Ar/O<sub>2</sub> gas flow ratio of 1–4, ZnO films are produced at the initial stage and subsequently ZnO nanorods with diameters of 30–70 nm are generated.

#### Acknowledgments

This work was supported by grant No. R05-2001-000-00843-0 from the Basic Research Program of the Korea Science & Engineering Foundation.

#### References

1. A. M. MORALES and C. M. LIEBER, *Science* **279** (1998) 208.
2. H. DAI, E. W. WONG, Y. Z. LU, F. SHOUSHAN and C. M. LIEBER, *Nature* **375** (1995) 769.
3. J. F. WANG, M. S. GUDIKNEN, X. F. DUAN, Y. CUI and C. M. LIEBER, *Science* **293** (2001) 1455.
4. W. S. SHI, Y. F. ZHENG, N. WANG, C. S. LEE and S. T. LEE, *Appl. Phys. Lett.* **78** (2001) 3319.
5. *Idem.*, *J. Vac. Sci. Technol. B* **19** (2001) 1115.
6. Y. LI, G. W. MENG, L. D. ZHANG and F. PHILLIPP, *Appl. Phys. Lett.* **76** (2000) 2011.
7. M. H. HUANG, Y. WU, H. FEICK, N. TRAN, E. WEBER and P. YANG, *Adv. Mater.* **13** (2001) 113.
8. Y. W. WANG, L. D. ZHANG, G. Z. WANG, X. S. PENG, Z. Q. CHU and C. H. LIANG, *J. Cryst. Growth* **234** (2002) 171.
9. B. D. YAO, Y. F. CHAN and N. WANG, *Appl. Phys. Lett.* **81** (2002) 757.
10. C. K. XU, G. D. XU, Y. K. LIU and G. H. WANG, *Solid State Commun.* **122** (2002) 175.
11. W. I. PARK, D. H. KIM, S. W. JUNG and G. C. YI, *Appl. Phys. Lett.* **80** (2002) 4232.
12. Y. DAI, Y. ZHANG, Y. Q. BAI and Z. L. WANG, *Chem. Phys. Lett.* **375** (2003) 96.
13. Y.-S. CHANG and J.-M. TING, *Thin Solid Films* **398/399** (2001) 29.
14. J. J. WU and S. C. LIU, *Adv. Mater.* **14** (2002) 215.
15. K.-S. KIM, H. W. KIM and C. M. LEE, *Mater. Sci. Eng. B* **98** (2003) 135.
16. JCPDS-International Center for Diffraction Data, JCPDS-ICDD, 2000.

Received 5 January  
and accepted 14 July 2004